

# INFLUENCE OF DELAMINATION INTERFACE LOCATION ON COMPRESSION STRENGTH OF FULLY ISOTROPIC LAMINATES AFTER IMPACT.

Periyasamy Manikandan<sup>1</sup> and Christopher B. York<sup>2</sup>

<sup>1</sup> 8 Commonwealth Lane, #02-01, Singapore 149555

[ManikandanP@wigetworks.com](mailto:ManikandanP@wigetworks.com)

<https://www.wigetworks.com/>

<sup>2</sup> 10 Dover Drive, Singapore 138683, Singapore Institute of Technology, Singapore,

[christopher.york@singaporetech.edu.sg](mailto:christopher.york@singaporetech.edu.sg)

<https://www.singaporetech.edu.sg/directory/faculty/christopher-york>

**Keywords:** Compression Strength after Impact, Fully Isotropic Laminates

## ABSTRACT

An experimental study of low velocity impact and quasi-static indentation damage is presented. Three non-symmetric laminates have been developed to eliminate many of the constraints found in previous studies, which include hygro-thermally curvature stable or warp free behaviour, no ply clustering, precisely matched stiffness properties; the laminates differ only by delamination interface location. Damage response and preliminary residual compression strength data is provided for impact events over standard rectangular aperture and circular aperture test fixtures, from which the influence of ply angle orientation on damage evolution can be assessed. A standard quasi-isotropic laminate is also considered, which is a common datum used in many other studies. Preliminary non-destructive and destructive evaluation of the delaminating interface locations and their relation to residual strength are also provided.

## 1 INTRODUCTION

This article presents preliminary results from an experimental study on residual compression strength of fully isotropic laminates, after barely visible impact damage. Special consideration is given to the effect on the residual strength characteristics arising from the dispersion of delaminating interfaces, assumed to occur between adjacent 0/90 and +45/-45 layers. The laminate designs adopted have standard ply angles and are free from ply blocking or clustering, but due to their non-symmetric warp-free stacking sequences, they exhibit different residual strength depending upon choice of impacted surface, through either low velocity impact or quasi-static indentation and using impact fixtures with either a circular or standard rectangular aperture or cut out. In the absence of high-fidelity NDT inspection results, post impact sectioning of the specimens is also adopted to investigate the locations and extent of initial delaminating interfaces. Post compression-after-impact inspection is then used to assess the major delamination interface locations leading to failure.

Three laminate designs have been developed algorithmically [1] to ensure precisely matched isotropy in both bending and extensional stiffness. These designs represent 24-ply laminates, which comply with ASTM thickness guidelines [2], noting that the recommended symmetric baseline design, which has been extensively adopted by other investigators, is Quasi-Isotropic but possesses both bending orthotropy ( $D_{11} \neq D_{22}$ ) and bending-twisting ( $D_{16} = D_{26} \neq 0$ ) coupling. The effect of bending-twisting coupling has not previously been assessed against a baseline design that is free from such mechanical coupling. Hence the three fully isotropic designs presented here offer alternative baseline designs, together with several important characteristics.

The new isotropic designs possess standard ply angles 0, 90, +45 and -45, rather than free-form or distributed angles adopted by others [3,10], which produced only approximate stiffness matching through variation in ply angles. Non-standard angle-ply orientations were found to produce



It is well known that compressive after impact (CAI) strength is dependent on the number of delamination planes and their dispersal within the laminate and that larger delamination spread occurs as the number of interfaces is reduced, hence it remains to be seen whether the new isotropic design comparators can offer additional insights into how the number and/or dispersal effect on CAI strength in the absence of other influencing factors.

The choice of impacted surface in non-symmetric laminates may lead to potentially different damage evolution, noting that the potential delaminating interfaces identified in Table 1 appear to be symmetric within all stacking sequences, but neither of the 0/90 nor +45/-45 ply interfaces are themselves symmetrically dispersed. The dominant delamination interface locations may be further exacerbated by the geometry of the standard rectangular aperture, or cut out, over which the specimens are placed and impacted. Indeed, it is conceivable that the assessment of damage tolerance between competing laminates may be completely different if the shape of the cut out is circular rather than rectangular.

## 2 MATERIAL SELECTION

The material used in this study was GURIT SE84LV/HEC/150/400/37±3%. This high modulus, high volume fraction carbon fibre/epoxy prepreg was cured at 120°C, but can also be cured at temperature as low as 80°C. The material is a 150gsm unidirectional prepreg, giving rise to a cured (24-ply) laminate thickness of approximately 3.8mm.

SE 84LV is a Lloyds Register Certified epoxy, chosen as a very low viscosity system, making it suitable for a range of pressure moulding processes, as well as for face sheets in sandwich structures, bonded primarily with a toughened SA 80 adhesive film. This material system is often used for marine application to construct high speed light weight boats.

## 3 IMPACT TEST METHOD

In this study, a comparison is made between the 75 × 100mm rectangular aperture or cut out of the standard impact test fixture and an alternative fixture with a 75mm circular aperture, see Fig. 1. The impact is performed using a fully instrumented 16mm diameter tup, or striker, mounted on a Zwick/Roell Amsler HIT1100F drop weight tester.

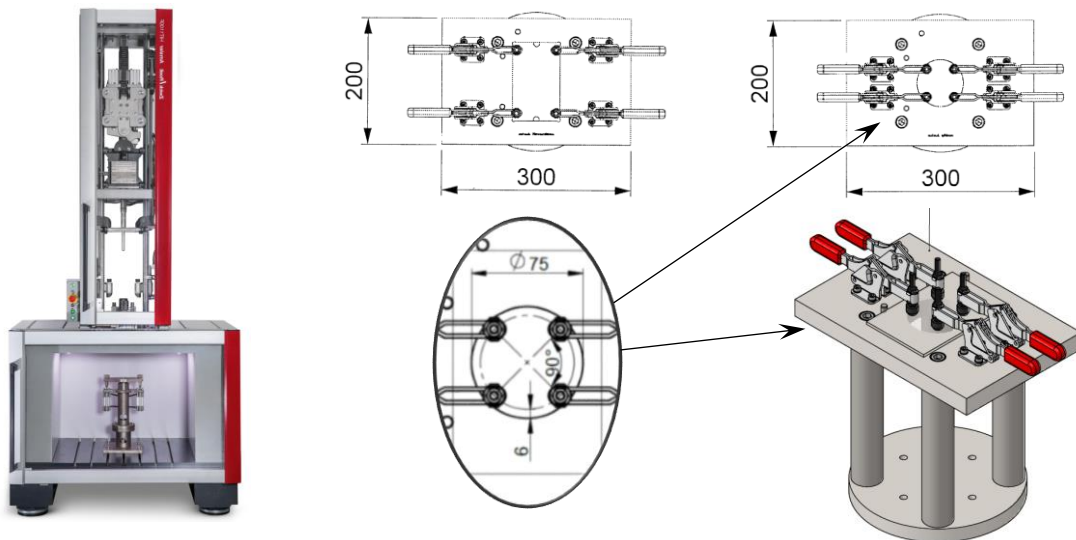


Figure 1: Zwick/Roell Amsler HIT1100F drop weight tester with standard CAI test fixture featuring a 125mm x 75mm rectangular cut out and modified impact fixture featuring a 75mm diameter circular aperture or cut out; rubber clamps are positioned radially at quarter points, 6mm inside the cut out to align with the positioning of clamps in the standard rectangular cut out.

Two energy levels were adopted in the study and these were compared to equivalent quasi-static indentation tests to try to understand the effects, if any, on the impact responses arising from the change

in geometry of the aperture, particularly when dominated by flexural and shear waves. These energies were informed by an earlier study [3], which demonstrated an abrupt change in indentation depth, used as a measure of barely visible impact damage, at 20J, in the ASTM sample adopted here for comparison purposes, hence 15J and 25J were chosen to avoid this transition point.

The 15J energy was generated by a 5kg mass falling from a height of 278mm, with an impact velocity of 2.335m/s, whereas the 25J energy was generated by the same mass falling from a height of 464mm, with an impact velocity of 3.017m/s.

The effect of using the Airbus standard, described elsewhere [6] as having clamps positioned over the platen of the impact fixture, 6mm away from the edge of the aperture or cut out, rather than positioned inside, in accordance with the ASTM standard [2], raises concerns about the effect of the clamp positions, during the impact event. A rotational restraint is introduced when the clamps are positioned outside the aperture or cut-out region, but such effects do not appear to have been investigated, except to note that the maximum delamination areas were greater than those recommended in the standard for the suggested impact energy.

Quasi-static indentation (QSI) tests were performed using both the rectangular and circular (not included in the current article) aperture because it has been shown that such tests can provide meaningful insight into the damage events occurring during a low velocity impact. Quasi-static indentation tests by others [8] adopted a smaller 50mm diameter circular aperture.

#### 4 NON DESTRUCTIVE AND DESTRUCTIVE INSPECTION

High fidelity C-Scans were unavailable at the time of publication, but the preliminary results, illustrated in Fig. 2, offer an insight into the difference in damage size and shape between the three laminate designs. The three laminates, ISO-1, ISO-2 and ISO-3, were impacted on either the bottom (B) or top (T) surface, as defined for the stacking sequence listings in Table 1, with 25J impact energy over either rectangular (R) or circular (C) apertures. The damage size does seem consistent with other studies [5], and is seen to be confined within the aperture region and generally does not exceed the diameter of the impactor. Moreover, damage is more concentrated on the circular samples compared to the rectangular samples because the area of circular aperture is smaller thus affecting bending deformation.

The preliminary C-Scan results do not offer detail on the delamination locations, hence a small number of impacted specimens were sectioned by waterjet cutting for inspection. The sectioning removed a 50 x 75mm quadrant or corner from the 100 x 150mm plate specimen to allow inspection of the cross-section through the impact zone exposed along the centre-line axes of the specimens.

The ISO-1, ISO-2 and ISO-3 specimens shown in Fig. 3 were impacted on the bottom (B) surface, defined in the stacking sequence listings in Table 1, with 15J impact energy over a rectangular (R) aperture, resulting in visible failure of the top surface plies. Details of the dominant delamination locations are made visible using a fluorescent dye penetrant. These images allow comparison of the predicted location of the potential delaminating interfaces, with those indicated alongside the stacking sequences in Table 1, noting that the impact is on the bottom surface, hence the fibre breakage is seen on the top surface.

Only one section is illustrated for the case of impact over the circular (C) aperture, corresponding to the ISO-3-B-15J-C specimen, which appears to have a larger number of delamination regions than expected in the vicinity of the impact, but highlights the two major 0/90 and 45/-45 interface locations at third point locations through the thickness, especially away from the impact region; these are also dominant in the ISO-3-B-15J-R, impacted over the rectangular aperture. The extent of the delamination is unclear given that the sectioning does not necessarily align with the direction in which the damage has propagated. There does appear to be major delamination of the 0/90 interface just below the top surface, i.e., the non-impacted surface.

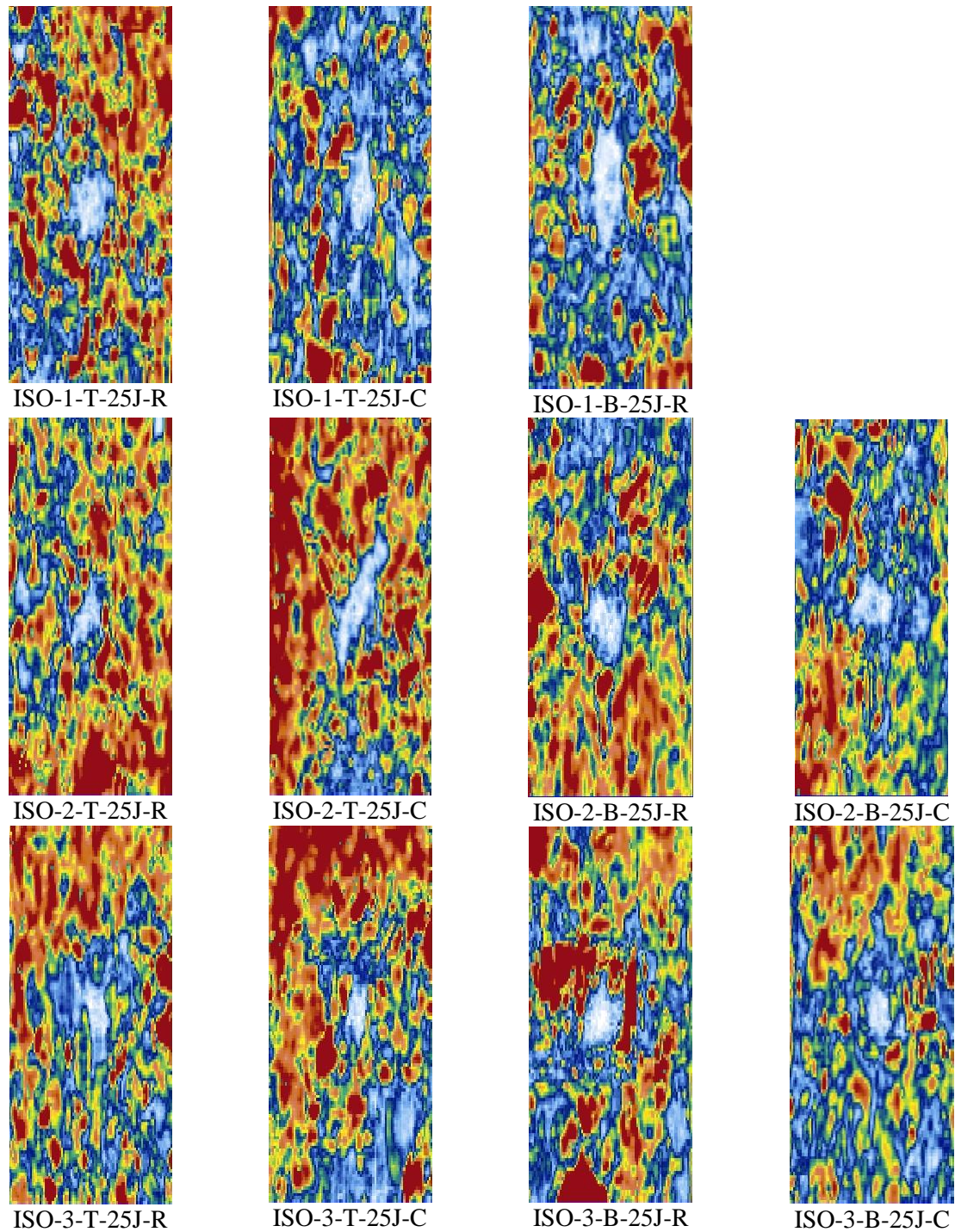


Figure 2: C-Scan images for the three designs representing a 80 x 120mm central region of the specimen; white areas indicate the extent of the impact damage.

The ISO-2-B-15J-R specimen contains four potential delamination locations forming a zone around each of the third point locations through the thickness, extending outward to the quarter point, which is the location of the most extensive visible delamination. Manufacturing defects are also apparent.

The ISO-1-B-15J-R specimen contains four potential delaminating locations within a zone ranging from the laminate surface down to quarter depth, as well as three locations within a zone at the laminate mid-plane. Delamination is visible in each of these zones.

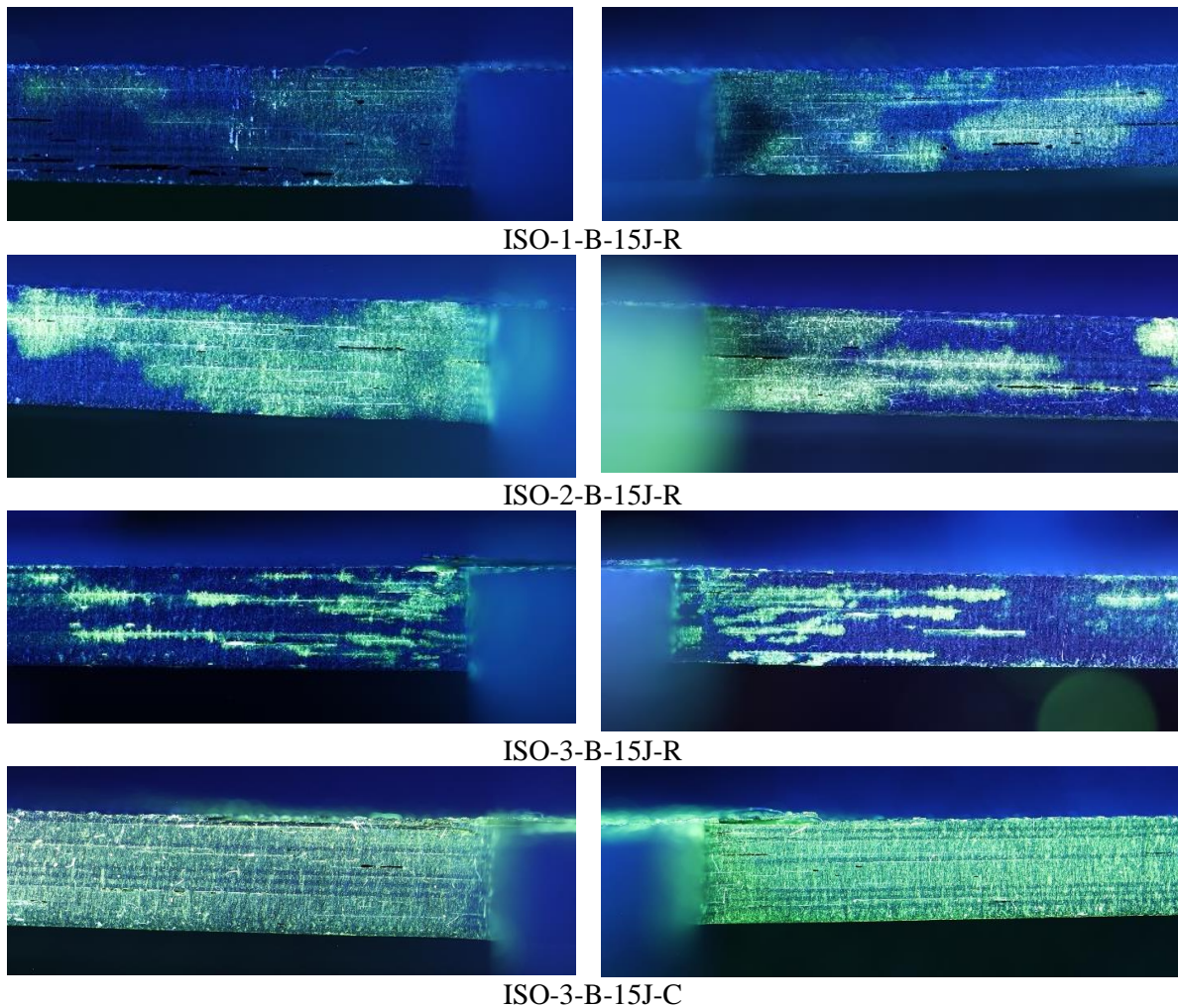


Figure 3: Cross-sections through the specimens subject to a Bottom (B) surface impact of 15J over Rectangular (R) and Circular (C) test apertures after waterjet removal of a 50 x 75mm quadrant, or quarter of the plate, to interrogate the dominant delamination interfaces, highlighted by fluorescent dye penetrant, on traverse and longitudinal centre-lines, respectively.

## 5 IMPACT DAMAGE RESPONSE

The results of Figs 4 - 6 represent a comparison between the Contact force against Contact Time and Impactor Displacement that reveal the differences in the damage signature, resulting from fibre failure or delamination at each individual drop in contact force, where the former causes abrupt change in contact force while the latter induces small high frequency oscillations along with marginal decrement of slope, respectively.

Figure 4 demonstrates that impact over a circular aperture produces in stiffer response (higher peak force, shorter contact time and smaller displacement) in comparison to the standard rectangular aperture. There is also a significant reduction in the flexural and shear wave response, which produces the oscillation in the curves as the contact force is increasing. The delamination threshold load, commonly defined as the first major drop in contact force, varies between 4.5 – 5.0kN for the three isotropic designs under 15J impact. The subsequent intermittent drops represent ply failures from the non-impacted side towards the impacted side with delamination damage at weak interface locations. Hence, this damage threshold will depend on which of the 0/90 and 45/-45 interfaces has the greater propensity for delamination.

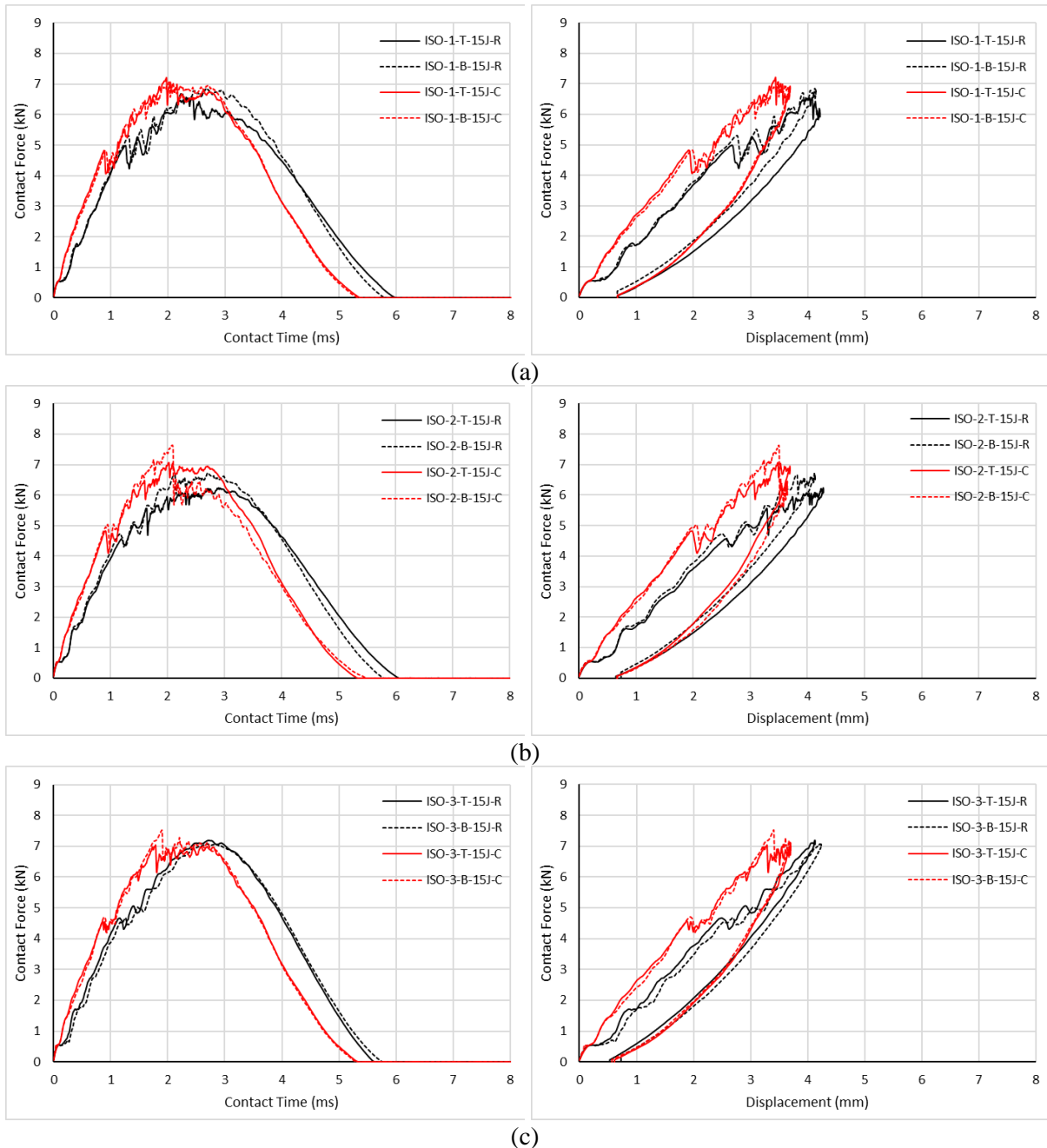


Figure 4: Force-time and Force-displacement responses for the three isotropic laminates of Table 1: (a) ISO-1; (b) ISO-2 and; (c) ISO-3, each subject to a Top (T) or Bottom (B) surface impact of 15J over Rectangular (R) or Circular (C) test apertures.

The variation resulting from impact on the top or bottom of the non-symmetric laminate is expected, since all laminates share a +45° top surface ply, but the bottom ply is different in all the designs, hence failure of the outer surface ply is expected to vary when impacted over a rectangular aperture but remain consistent when impacted over a circular aperture.

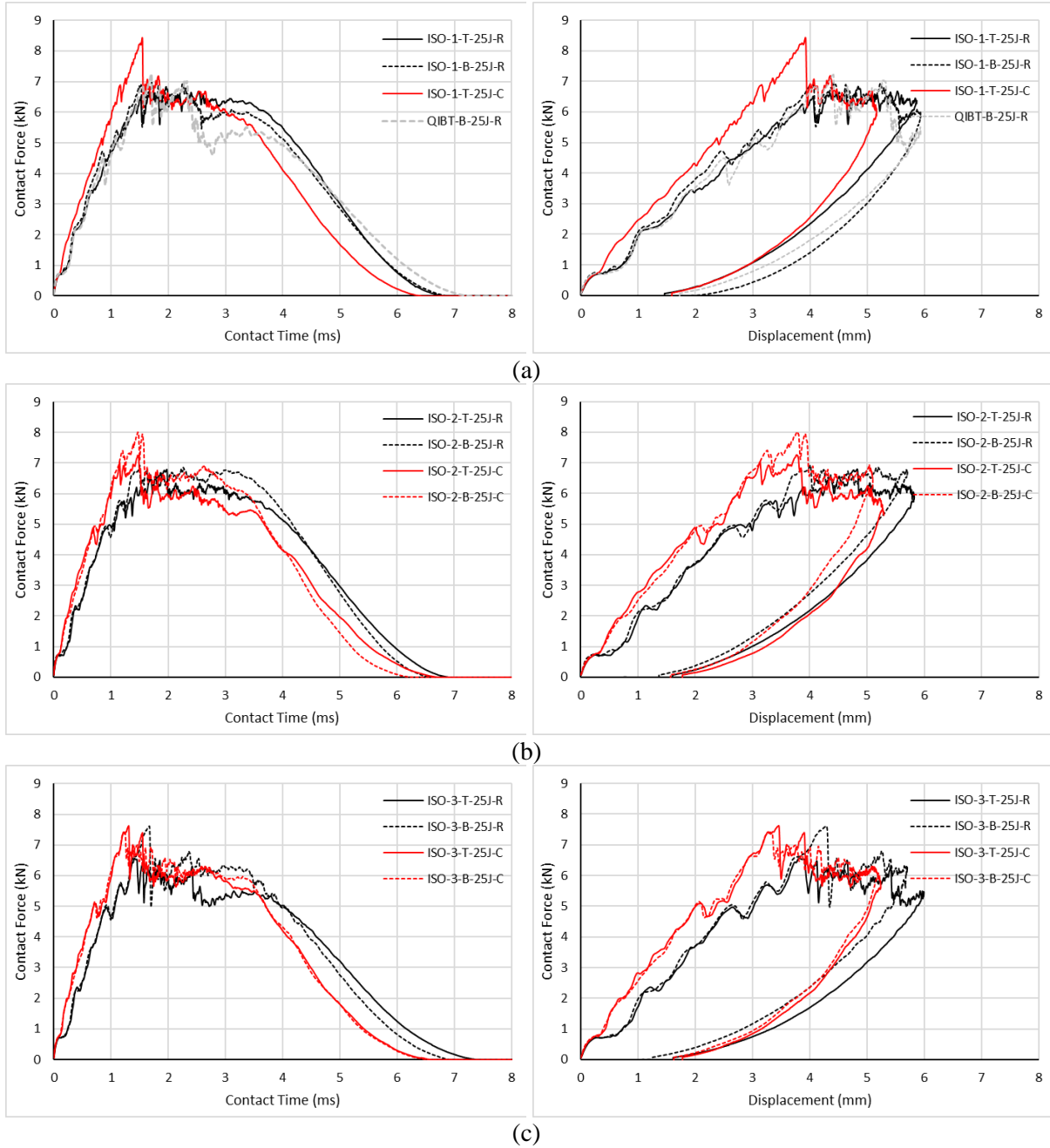


Figure 5: Force-time and Force-displacement responses for the three isotropic laminates of Table 1: (a) ISO-1, including the quasi-isotropic symmetric laminate (defined as QIBT in Table 1) recommended within the ASTM standard; (b) ISO-2 and; (c) ISO-3, each subject to a Top (T) or Bottom (B) surface impact of 25J over Rectangular (R) or Circular (C) test apertures.

Figure 5 demonstrates a similar set of results to those of Fig. 4, but subject to an impact energy of 25J. The results include a quasi-isotropic symmetric laminate (QIBT) recommended within the ASTM standard [2], which has a response comparable to the isotropic design, but shows a significant drop in contact force, which may be a result of the coupling behaviour between bending and twisting. The effect of the ply block in this design may also account for a reduction in damage tolerance.

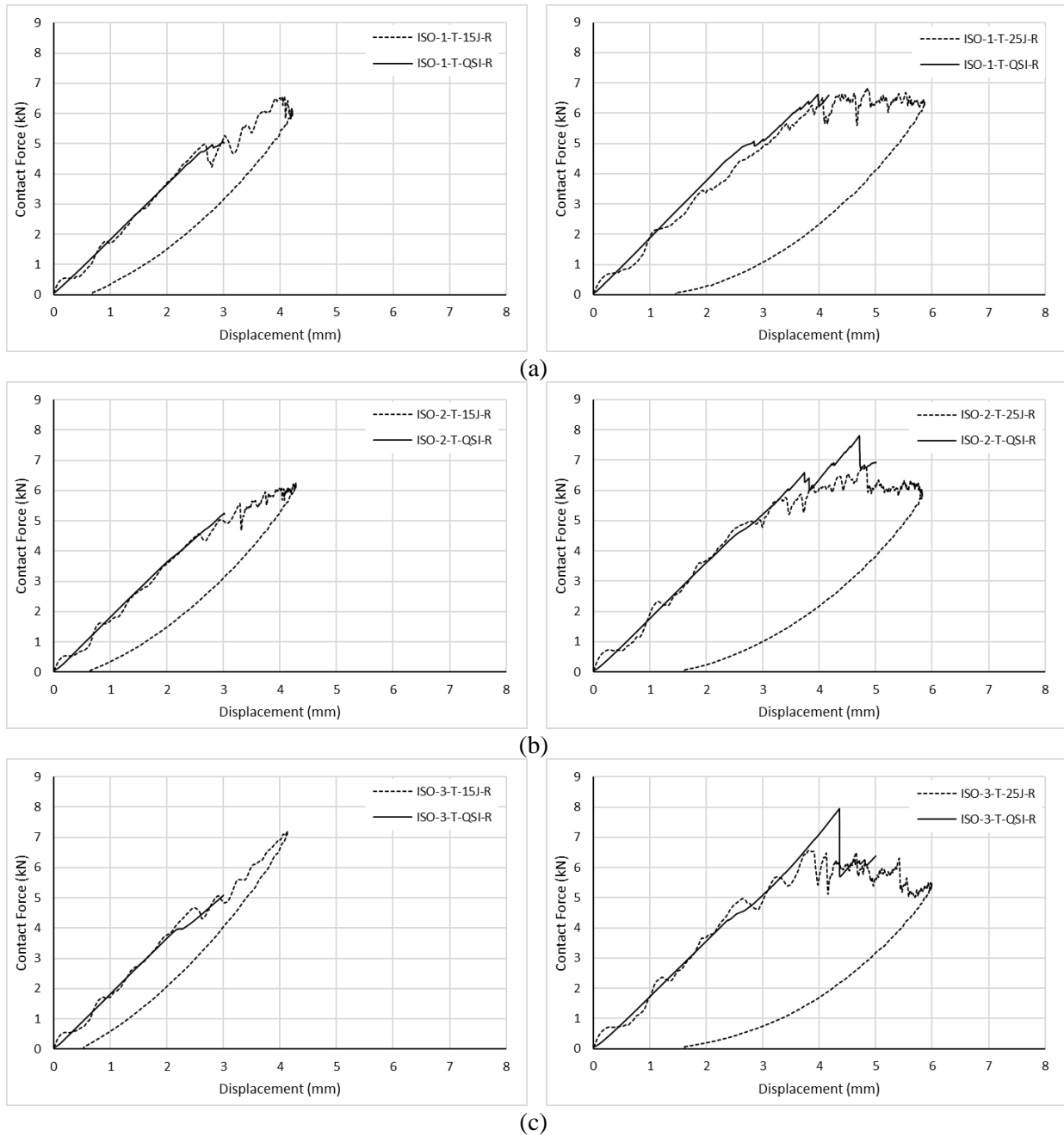


Figure 6: Comparison of force-displacement response subject to either a top (T) impact of 15J and 25J (broken lines) or equivalent 3mm and 5mm Quasi-Static-Indentation (solid line) over a Rectangular (R) test aperture for the isotropic laminates defined in Table 1: (a) ISO-1; (b) ISO-2 and; (c) ISO-3.

The QSI tests (1.25mm/min loading rate) with 3 and 5mm deflections, illustrated in Fig. 6, provide some degree of correlation between the test results for low velocity impact of 15J and 25J, respectively, using an identical indenter to that used for impact loading.

*Note on clamping:* The perimeter edges of the plates were observed to lift from the platen during the QSI test, suggesting that clamps securing the plate over the platen (6mm from the edge of the cut out) introduce a constraint that is not present in the ASTM standard fixture, in which clamps secure the plate over the cut out (6mm from the edge).

*Note on static indentation:* Indentations we seen to begin at above 4kN, as seen by a change in gradient of the load-deflection curve that is consistent with low velocity impact response. It should also be noted that an indentation load of 16kN was required to produce a 1mm indentation under a modified QSI test, in which the specimen was placed on a solid plate, rather than the test fixtures with cut outs.

## 6 COMPRESSION STRENGTH AFTER IMPACT

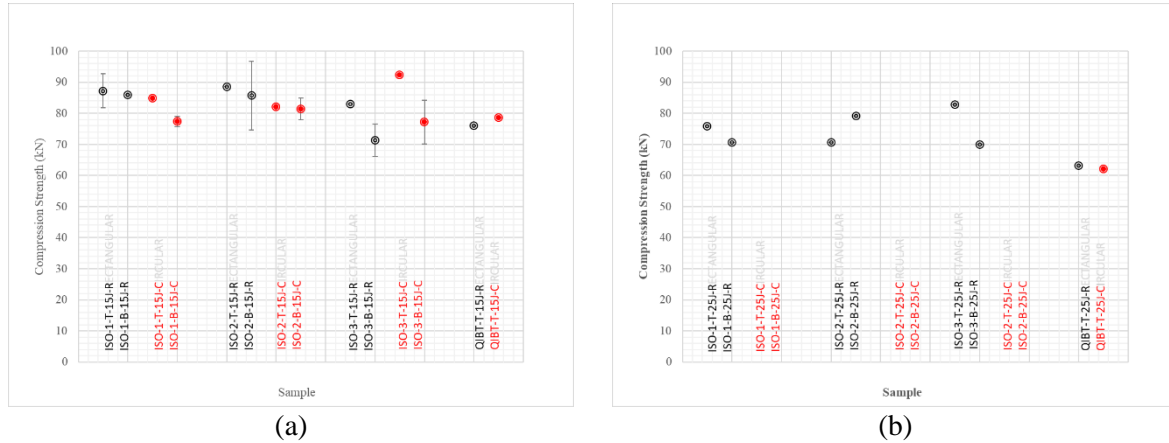


Figure 7: Compression strength after impact for the three isotropic designs (ISO-1,2,3) of Table 1, including the quasi-isotropic (QIBT) design recommended within the ASTM standard [2], and subject to a Top (T) or Bottom (B) surface impact of 15J or 25J over Rectangular (R) or Circular (C) test apertures.

Figure 7 results demonstrate that regardless of aperture shape, compression after impact (CAI) strength of samples impacted on the bottom surface are marginally lower than the samples impacted on top surface. For the three ISO samples, the ISO-3 design, with four dispersed critical delamination interfaces, shows the most significant drop in the CAI strength between all impacted samples whether it be top or bottom surface impact irrespective of the impact aperture used.

The CAI residual strength for ISO-1 and ISO-2 samples are in the range between 80-90 kN while for ISO-3 samples the ranges is between 70-90. From the post-mortem inspections shown in Figs 8 - 11, the delamination damage on ISO-1 and ISO-2 samples are highly interlinked between interfaces since they are close to each other and cause minor delamination damage on every interface. However, on ISO-3 samples where the critical delamination interfaces are far away from each other the delamination damage is more concentrated on these interfaces; the axial compression load is effectively carried through multiple sub-laminates which are stacked one above the other. For the ISO-3 samples impacted over the circular aperture, which results in severe concentrated fiber damage within the impacted zone, the resulting sub-laminates are unable to sustain the axial load and thus register very low residual strength compared to ISO-3 samples impacted over the rectangular aperture.

Figures 8 - 11 offer comparisons of post compression after impact damage on the two sides of each specimen, based on initial impact or quasi-static indentation corresponding to similar maximum deflection during the impact event of 3 and 5mm for 15J and 25J, respectively. The delamination locations correlate, in general, to those indicated in Table 1 as potential delaminating interfaces. The extent of the delamination and damage morphology along the width of the sample shows some degree of mismatch which is explained by the fact that the damage induced by the impact event is primarily driven by the fibre direction.



Figure 8: Comparison of fracture mechanisms for the 3 isotropic designs (ISO-1 – ISO-3) following bottom surface (B) impact of 15J using the standard rectangular aperture (R) impact fixture, viewed from the left and right side respectively.

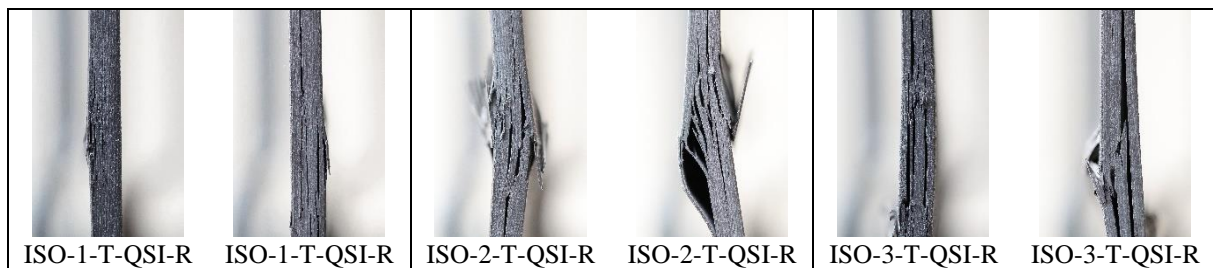


Figure 9: Comparison of fracture mechanisms for the 3 isotropic designs (ISO-1 – ISO-3) following top surface (T) quasi-static indentation (QSI) of 3mm over the standard rectangular aperture (R) impact fixture, viewed from the left and right side respectively.

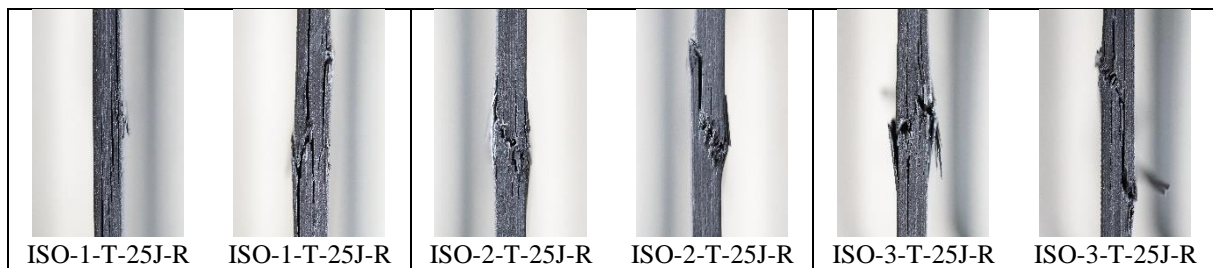


Figure 10: Comparison of fracture mechanisms for the 3 isotropic designs (ISO-1 – ISO-3) following top surface (T) impact of 25J using the standard rectangular aperture (R) impact fixture, viewed from the left and right side respectively.

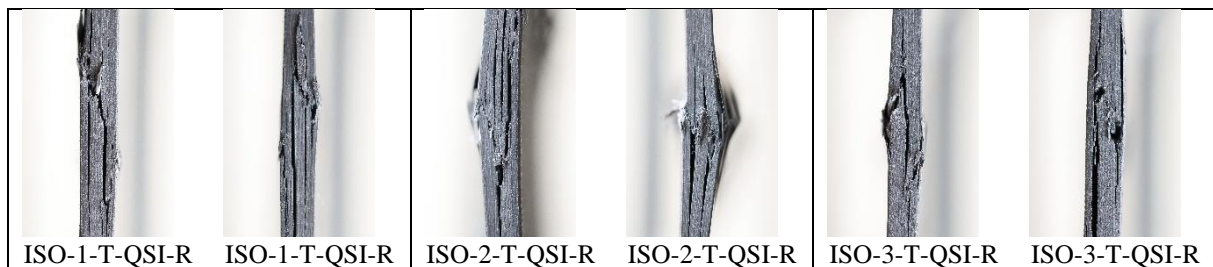


Figure 11: Comparison of fracture mechanisms for the 3 isotropic designs (ISO-1 – ISO-3) following top surface (T) quasi-static indentation (QSI) of 5mm over the standard rectangular aperture (R) impact fixture, viewed from the left and right side respectively.

## 7 CONCLUDING REMARKS

Preliminary results for compression strength after impact have been presented for a new set of datum designs with fully isotropic properties. The designs have standard ply angles and are free from ply blocking or clustering. The designs are also non-symmetric yet are hygro-thermally curvature stable or warp free, and as a result offer the potential for new insights for improved damage tolerance.

As in previous studies, the need for more experimental tests seems to be a common requirement to adequately support any conclusions drawn, given that the repeatability of the CAI tests were found to be less consistent than the impact tests.

## ACKNOWLEDGEMENTS

The authors are grateful for support from the Ministry of Education under grant (R-MOE A403-G011) and to the Instituto de Pesquisas Tecnológicas for providing the preliminary c-scan images.

## REFERENCES

- [1] C. B. York, A unified approach to the characterization of coupled composite laminates: benchmark configurations and special cases, *Journal of Aerospace Engineering*, **23**(4), 2010, pp. 219-242 (doi: 10.1061/(ASCE)AS.1943-5525.0000036).
- [2] ASTM D7136/D7136M-15 *Standard Test Method for Measuring the Damage Resistance of a Fiber-Reinforced Polymer Matrix Composite to a Drop-Weight Impact Event*, ASTM International, West Conshohocken, PA. 2015.
- [3] T.A. Sebaey, E.V. González, C.S. Lopes, N. Blanco, J. Costa, Damage resistance and damage tolerance of dispersed CFRP laminates: Effect of ply clustering, *Composite Structures*, **106**, 2013, pp. 96–103 (doi:10.1016/j.compstruct.2013.05.052)
- [4] A. Sasikumar, J. Costa, D. Trias, E.V. González, S.M. García-Rodríguez, P. Maimí, Unsymmetrical stacking sequences as a novel approach to tailor damage resistance under out-of-plane impact loading, *Composites Science and Technology*, **173**, 2019, pp. 125-135 (doi: 10.1016/j.compscitech.2019.02.002).
- [5] A. Sasikumar, S.M. García-Rodríguez, J.J. Arbeláez, D. Trias, J. Costa, On how unsymmetrical laminate designs with tailored ply clusters affect compression after impact strength compared to symmetric baseline, *Composite Structures*, **238**, 2020, 111958 (doi: 10.1016/j.compstruct.2020.111958).
- [6] E.V. González, P. Maimí, P.P. Camanho, C.S. Lopes, N. Blanco, Effects of ply clustering in laminated composite plates under low-velocity impact loading, *Composites Science and Technology*, **71**, 2011, pp. 805–817 (doi:10.1016/j.compscitech.2010.12.018)
- [7] ASTM D7137/D7137M-12 *Standard Test Method for Compressive Residual Strength Properties of Damaged Polymer Matrix Composite*, ASTM International, West Conshohocken, PA, 2012.
- [8] A. Wagih, P. Maimí, N. Blanco, J. Costa, A quasi-static indentation test to elucidate the sequence of damage events in low velocity impacts on composite laminates, *Compos Part A: Applied Science and Manufacturing*, **82**, 2016, pp. 180-189 (doi: 10.1016/j.compositesa.2015.11.041)
- [9] R.D. Martins, M.V. Donadon, S.F.M. Almeida, The effects of curvature and internal pressure on the compression-after-impact strength of composite laminates, *Journal of Composite Materials*, **50**, 2015, pp 1-24 (doi:10.1177/0021998315582079)
- [10] C.S. Lopes, O. Seresta, Y. Coquet, Z. Gurdal, P.P. Camanho, B. Thuis, Low-velocity impact damage on dispersed stacking sequence laminates. Part I: experiments. *Composite Science and Technology*, **69**, 2009, pp. 926-936.